

Nonclassical Radiation from Thermal Cavities in the Ultrastrong Coupling Regime

A. Ridolfo¹, S. Savasta², and M. J. Hartmann¹

¹*Physik Department, Technische Universität München, 85748 Garching, Germany*

²*Dipartimento di Fisica e Scienze della Terra, Università di Messina, I-98166 Messina, Italy*

(Dated: December 7, 2012)

Thermal or chaotic light sources emit radiation characterized by a slightly enhanced probability of emitting photons in bunches, described by a zero-delay second-order correlation function $g^{(2)}(0) = 2$. Here we explore photon-coincidence counting statistics of thermal cavities in the ultrastrong-coupling regime, where the atom-cavity coupling rate becomes comparable to the cavity resonance frequency. We find that, depending on the system temperature and coupling rate, thermal photons escaping the cavity can display very different statistical behaviors, characterised by second-order correlation functions approaching zero or greatly exceeding two.

PACS numbers: 42.50.Pq, 42.50.Ar, 85.25.-j, 03.67.Lx

Thermal radiation deserves a special place in modern physics. In the search for a solution to the discrepancies between the observed energy spectrum of thermal radiation and the predictions of classical theory, Planck was led to introduce the revolutionary concept of quanta [1]. Thermal or chaotic light sources emit radiation that is characterized by an enhanced probability of emitting photons in bunches [2]. In the course of the successful attempt at explaining such effect, Glauber established the basis of quantum optics [3, 4]. Even more recently the study of thermal emission has continued to provide amazing results. A thermal light-emitting source is often presented as a typical example of an incoherent source. However, it has been shown that the field emitted by a thermal source made of a polar material is enhanced by more than four orders of magnitude and displays first-order coherence in the near-field zone [5]. Moreover, by introducing a periodic microstructure into such a polar material, a thermal infrared source can be fabricated that displays first-order coherence over large distances [6]. While first-order coherence and spectral properties of thermal sources can be manipulated and tailored, their second-order coherence is known to be completely absent [4] resulting in the small bunching described by $g^{(2)}(0) = 2$.

Here we investigate photon-coincidence counting statistics of thermal cavities in the ultrastrong-coupling regime, where the strength of the interaction Ω_R between an emitter and the cavity photons becomes comparable to the transition frequency of the emitter ω_x or the frequency of the cavity mode ω_0 . Cavities with ultrastrong light-matter interactions, are attracting interest both in semiconductor and superconducting systems, due to the possibility of manipulating the physical properties of the cavity quantum electrodynamic ground state [7–12].

The photon statistics of chaotic sources (like thermal cavities) and also of lasers can be explained classically. In contrast, strongly nonlinear photonic systems can emit photons one by one well separated in time from each other when excited coherently or operating very far from thermal equilibrium. For the systems considered so far,

such scenario is however known to not persist when the coupled system is driven by thermal noise induced by reservoirs at a given temperature T . Indeed, the standard quantum optics Master Equation (ME), generally used to study the dynamics of cavity QED systems [13], predicts for such systems $g^{(2)}(0) = 2$ independently of temperature and coupling strength. The interaction between atoms and cavity photons is most often neglected when considering the coupling of this system with an environment. Recently it has however been shown that this simplification, which leads to the standard quantum optics ME, can give origin to unphysical effects in the ultrastrong coupling regime [14]. Another key issue is the failure of standard quantum optical normal order correlation functions to describe photodetection experiments for such systems [15, 16]. The theoretical treatment of this regime thus requires a description that goes beyond the standard techniques of quantum optics.

By exploiting generalized correlation functions as introduced in [16] and a ME that fully takes into account the qubit-resonator coupling [14], we investigate the photon-coincidence counting statistics of thermal sources for arbitrary light-matter coupling. The system that we investigate consists of a single mode resonator coupled to a two-level quantum emitter. Each subsystem is coupled to independent thermal baths of harmonic oscillators at the same temperature T . We concentrate on the zero-detuning $\omega_0 = \omega_x$ and low-temperature cases, where more striking deviations from standard results appear. We have corroborated the generality of our findings by confirming that similar results are found for one cavity mode coupled to multiple emitters or one emitter coupled to multiple cavity modes, see supplementary material [29].

A particularly well suited technology for such an experiment are superconducting circuits [17, 18] which have recently emerged as an excellent platform for microwave on-chip quantum-optics experiments and where second-order correlation function measurements for quantum [19–21] and low temperature thermal fields [22] have been

performed using quadrature amplitude detectors.

Model - The cavity QED system that we explore consists of a single-mode resonator in interaction with a two level system (TLS). This interacting system can be described by the Rabi Hamiltonian (assuming $\hbar = 1$),

$$H = \omega_0 a^\dagger a + \omega_x \sigma^+ \sigma^- + g(a + a^\dagger)(\sigma^- + \sigma^+) \quad (1)$$

where ω_0 and ω_x are the cavity and TLS bare frequencies, g is the coupling strength, while $a(a^\dagger)$ and $\sigma^- (\sigma^+)$ denote the annihilation (creation) operators for the cavity and TLS. Since we are interested in probing photon-coincidence statistics for arbitrary light-matter interactions where the contribution of the counter rotating terms cannot be neglected, we do not make use of the rotating wave approximation (RWA) [31]. Recently, it was shown that in the limit of very large coupling, the ground state and the first excited state of this system can become quasidegenerate [23–25].

In order to study thermal emission as well as the statistics of thermal photons we calculate the normal-order correlation functions of the output field. Standard normal order correlation functions were recently shown to not correctly describe the emission properties and photon statistics of systems in the ultrastrong coupling regime [16]. For example, an application of the standard procedure to the ultrastrong-coupling regime would predict an unphysical stream of output photons even for a zero-temperature system: $\langle a^\dagger a \rangle_{T=0} = \text{Tr}[a^\dagger a \rho_{T=0}] \neq 0$. Following [16], we employ correlation functions for the output fields that are valid for an arbitrary coupling strength by expressing the cavity field $X = X_0(a + a^\dagger)$ (X_0 is the rms zero-point field-amplitude) in the atom-cavity dressed basis. In particular, the set-up we have in mind is equivalent to the emission of a thermalized black-box, whose output is coupled to the vacuum of a one-dimensional waveguide. In this case, by defining $a_{\text{out}}(t)$ and $a_{\text{in}}^{\text{vac}}(t)$ as the output and input operators, the input-output relations become, $a_{\text{out}}^+(t) = a_{\text{in}}^{\text{vac}}(t) - i\sqrt{\gamma_a} \dot{X}^+$ [16], where X^+ is the positive frequency component of the cavity field X . The positive and negative frequency components ($X^- = (X^+)^{\dagger}$) can be derived by expanding the operators in the dressed state basis, namely the eigenstates $|j\rangle$ of H as in Eq. (1) ordered according to increasing eigenenergies ω_j . Specifically, the time derivative of X^+ can be expressed as $\dot{X}^+ = -i \sum_{j,k>j} \Delta_{kj} X_{jk} |j\rangle \langle k|$ where $X_{jk} = \langle j|X|k\rangle$ and $\Delta_{kj} = \omega_k - \omega_j$. According to these input-output relations and for input fields in vacuum, the normalized second order correlation function for the output field can be expressed as

$$g^{(2)}(\tau) = \lim_{t \rightarrow \infty} \frac{\langle \dot{X}^-(t) \dot{X}^-(t+\tau) \dot{X}^+(t+\tau) \dot{X}^+(t) \rangle}{\langle \dot{X}^-(t) \dot{X}^+(t) \rangle^2}. \quad (2)$$

Results - The thermal-equilibrium zero-delay correlation function $g^{(2)}(0)$ can be directly calculated once the thermal equilibrium density-operator is known [28]. For

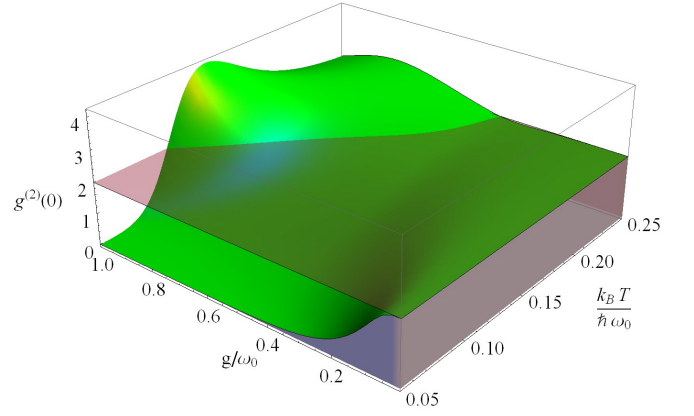


FIG. 1: (color online) $g^{(2)}(0)$ calculated as function of the temperature and coupling strength. The results are obtained at resonance ($\omega_0 = \omega_x$) and for a steady-state imposing thermal equilibrium between cavity and TLS, i.e. $T_a = T_x$. Notably, at thermal equilibrium, statistical properties are independent of the damping rates. For comparison we show, the plane of $g^{(2)}(0) = 2$ which indicates the value that would result from a conventional ME, where a RWA is performed.

a system at thermal equilibrium, statistical properties are related to the density matrix of the canonical ensemble, that is the most general way to describe such thermalized interacting systems. Once H is in its diagonal form, the density matrix of the canonical ensemble reduces to,

$$\rho_T = \frac{e^{-(\epsilon_j/k_B T)}}{\mathcal{Z}} \delta_{ij}, \quad (3)$$

where ϵ_j is the j -th eigenvalue of H , δ_{ij} the Kronecker delta function, and $\mathcal{Z} = \sum_j \exp(-\epsilon_j/k_B T)$ the partition function. Figure 1 displays the thermal-equilibrium zero-delay correlation function $g^{(2)}(0)$ as a function of the effective coupling g/ω_0 and temperature calculated at zero detuning ($\omega_0 = \omega_x$). The calculated $g^{(2)}(0)$ exhibits striking differences from the standard value of $g^{(2)} = 2$. Of particular interest is the region with large effective coupling $g/\omega_0 > 0.4$ and low temperature $k_B T/\omega_0 < 0.1$ where $g^{(2)}(0)$ becomes very small. Such highly nonclassical behavior of thermal photons opens the perspective towards the realization of thermal sources of single photons in circuit QED. This anomalous behavior originates from the tendency of the interacting quantum system towards the vacuum degeneracy for large couplings. Specifically for increasing coupling the energy of the first excited state converges towards that of the ground state, while the other energy levels remain well separated from that doublet (see Fig. 2b). Hence, at sufficiently low temperature, only the first excited state is significantly populated by thermal noise ($(\omega_i - \omega_0)/kT$ is non-negligible only for $i = 1$). At the onset of vacuum degeneracy, the ground and first excited state are quantum superpositions with multi-photon components [24] and at first sight one might expect to observe bunching effects. However such pho-

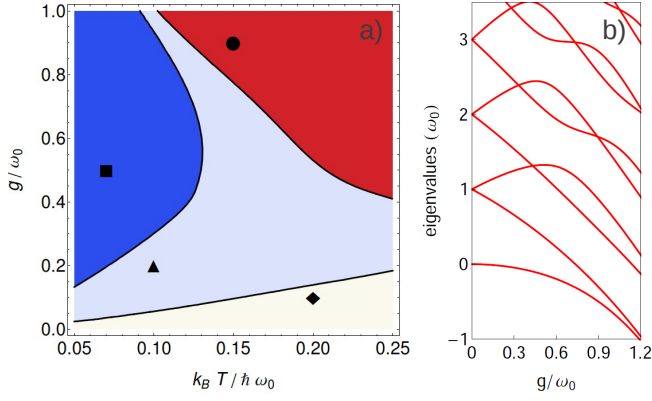


FIG. 2: (color online) **a)** Contourplot of $g^{(2)}(0)$ calculated with the same parameters as Fig. 1. Here one can distinguish four regions: i) milky, with $1.999 < g^{(2)}(0) < 2$ corresponding to the standard thermal result, ii) gray, for $1 < g^{(2)}(0) < 1.999$, iii) blue, with the sub-Poissonian values $g^{(2)}(0) < 1$ and iv) red, with a $g^{(2)}(0) > 2$. The markers in these four regions are useful to characterise the different behaviors of $g^{(2)}(\tau)$ and their $(g/\omega_0, k_B T / \hbar \omega_0)$ values are: diamond (0.1, 0.2), triangle (0.2, 0.1), square (0.5, 0.07), circle (0.9, 0.15). **b)** Energy eigenvalues of H as in equation (1) as a function g/ω_0 .

tons are mostly virtual and the use of generalized normal order correlation functions shows that the transition $|1\rangle \rightarrow |0\rangle$ can only emit one physical photon at a time resulting into $g^{(2)} \ll 1$.

For large effective couplings and higher temperatures $g^{(2)}(0)$ becomes larger than the standard value, $g^{(2)}(0) = 2$. Also this behaviour can be understood from the energy levels in Fig. (2b). In particular at $g/\omega_0 \simeq 0.45$, a crossing between levels 2 and 3 ($2 \leftrightarrow 3$) occurs. Moreover the energy ω_3 lowers further for increasing g , so that, if temperature is not too low, thermal noise can populate the state $|3\rangle$, giving rise to an increase of the second order correlation function $g^{(2)}(0)$ due to the cascade transitions $|3\rangle \rightarrow |1\rangle \rightarrow |0\rangle$. An overview of the behaviors of $g^{(2)}(0)$ is given in the contour plot of Fig. 2, where four different regions are displayed: i) a region for small g/ω_0 (labelled by the diamond) where the standard thermal result $g^{(2)} \approx 2$ is recovered (here $1.999 < g^{(2)}(0) < 2$) and which broadens for increasing temperatures; ii) a sub-Poissonian or nonclassical region with $g^{(2)} < 1$ (square) in the ultrastrong coupling regime and for sufficiently low temperatures; iii) a region with an intermediate regime (triangle) with $1 < g^{(2)}(0) < 2$; and iv) a super-Poissonian region (circle) beyond the standard value $g^{(2)} = 2$ for very large coupling and higher temperatures. We note here that a calculation of $g^{(2)}(0)$ within the rotating wave approximation and using the standard quantum optics ME [13] would always yield the value $g^{(2)}(0) = 2$, regardless of the coupling strength and the temperature.

Although the steady state properties can be obtained from Eq. (3), a comprehensive description of the time dependent dynamics is possible only using the ME approach. While zero-delay correlation function can be directly inferred from the thermal density operator, a description of the time dependent dynamics of the open quantum system is required to calculate the time-delayed second order correlation function $g^{(2)}(\tau)$. A viable description of system-bath interactions typically requires an expansion in the system bath coupling. A suitable way to perform this perturbative expansion consists in writing the Hamiltonian in the basis of its eigenstates $|j\rangle$. In this way we obtain the following ME [14, 26]

$$\dot{\rho}(t) = i[\rho(t), H] + \mathcal{L}_a \rho(t) + \mathcal{L}_x \rho(t), \quad (4)$$

where \mathcal{L}_a and \mathcal{L}_x are Liouvillian superoperators describing the losses and the thermal feeding of the system. They read, $\mathcal{L}_c \rho(t) = \sum_{j,k>j} \Gamma_c^{jk} \bar{n}(\Delta_{kj}, T_c) \mathcal{D}[|k\rangle\langle j|] \rho(t) + \sum_{j,k>j} \Gamma_c^{jk} (1 + \bar{n}(\Delta_{kj}, T_c)) \mathcal{D}[|j\rangle\langle k|] \rho(t)$ for $c = a, \sigma^-$ with $\mathcal{D}[O]\rho = \frac{1}{2}(2O\rho O^\dagger - \rho O^\dagger O - O^\dagger O\rho)$. The relaxation coefficients $\Gamma_c^{jk} = 2\pi d_c(\Delta_{kj}) \alpha_c^2(\Delta_{kj}) |C_{jk}^c|^2$ depend on the spectral density of the baths, $d_c(\Delta_{kj})$, and the system-bath coupling strength, $\alpha_c(\Delta_{kj})$, at the respective transition frequency $\Delta_{kj} = \omega_k - \omega_j$ as well as on the transition coefficients $C_{jk}^c = -i\langle j|(c - c^\dagger)|k\rangle$ ($c = a, \sigma^-$). $\bar{n}(\Delta_{kj}, T_c)$ is the thermal population at frequency Δ_{kj} and T the temperature. In all examples reported in this work, we consider a cavity that couples to the momentum quadratures of fields in one-dimensional output waveguides, assuming that i) the spectral density $d_c(\Delta_{kj})$ is constant and $\alpha_c^2(\Delta_{kj}) \propto \Delta_{kj}$ ii) the cavity-TSL system is at the thermal equilibrium, i.e. $T_a = T_x$. Hence the relaxation coefficients reduce to $\Gamma_c^{jk} = \gamma_c(\Delta_{kj}/\omega_0) |C_{jk}^c|^2$, where γ_c are the standard damping rates. These assumptions correspond to a cavity coupled to a one dimensional output waveguide as e.g. in circuit-QED. In the ME (4) we neglect contributions of dephasing noise and Lamb shifts as they do not affect significantly our findings. A first result worth mentioning is that the steady state solution of Eq. (4) reproduces the thermal density matrix Eq. (3). This confirms that the present approach is able to describe correctly the system thermalization, thus providing a validation of Eq. (3). We then solve Eq. (4) using as initial conditions the steady-state collapsed density matrix $\tilde{\rho}(t) = \dot{X}^+ \rho(t) \dot{X}^-$ and use $\tilde{\rho}(t + \tau)$ to calculate $g^{(2)}(\tau)$ via the quantum regression theorem.

Figure 3 displays $g^{(2)}(\tau)$ for temperatures and couplings corresponding to the reported markers in Fig. 2 and for $\gamma_a = \gamma_x = 0.01\omega_0$. It is worth to notice the appearance of oscillations in the triangle and diamond regions. Such oscillations arise from the superposition of the possible decay channels. In fact, for these values of the coupling strength, the separation between the energy levels is not high enough to suppress thermal occupation of higher excited states. Hence decays from upper energy

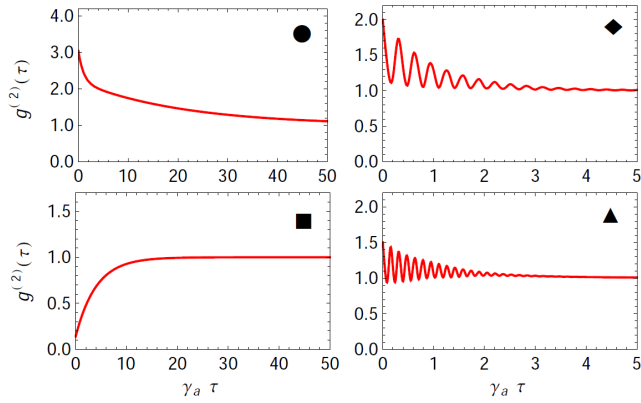


FIG. 3: (color online) $g^{(2)}(\tau)$ calculated for couplings and temperatures corresponding to the markers in Fig. 2. Here the damping rates are $\gamma_a = \gamma_x = 0.01\omega_0$.

manifolds into lower excited states are possible. In this way, e.g. the third excited energy level can decay into the second or into the first, enabling a quantum superposition of possible pathways and giving rise to this kind of oscillating behavior. This explanation is corroborated by the fact that the frequency of the oscillations corresponds exactly to Δ_{12} , i.e. the energy difference between the first and the second excited state of H . Yet, in the square region $g^{(2)}(\tau)$ is almost zero and it behaves as for a usual TLS, moreover the oscillations in τ are suppressed by the low thermal noise and by the great separation in energy between the energy eigenvalues. Instead, the $g^{(2)}(\tau)$ in the dot region shows a slow decay for large τ which is in agreement with the extremely narrow linewidth of the transition between the first excited and the ground state ($|1\rangle \rightarrow |0\rangle$) (see Fig. 4). In fact, owing to the remarkable lifetime difference between the transitions $|1\rangle \rightarrow |0\rangle$ and $|3\rangle \rightarrow |1\rangle$, the probability to measure a second photon at time τ is substantial as the first detected photon emerges from the decay of $|3\rangle$ into $|1\rangle$ and the second from the decay of $|1\rangle$ into $|0\rangle$. The latter is delayed due to the long lifetime of the transition $|1\rangle \rightarrow |0\rangle$. For this reason, the $g^{(2)}(\tau)$ in the red region remains bunched for such a long time. Such behavior is a consequence of the spectral density of the bath that, being a linear function of the frequencies, tends to narrow the spectral linewidth of the lower resonances.

Thermal emission is also characterized by its power spectrum, i.e. the Fourier transform of the two time correlation $S(\omega) \propto \lim_{t \rightarrow \infty} 2\Re \int_0^\infty \langle \dot{E}^-(t) \dot{E}^+(t+\tau) \rangle e^{i\omega\tau} d\tau$. We exploit again the quantum regression theorem to calculate the relevant two-time correlation function. Fig. 4 shows calculations of $S(\omega)$ with the same parameters as used in Fig. 3 and the corresponding values of temperature and couplings for the different markers as reported in the caption of Fig. 2. As expected the heights of the spectra increase for increasing temperature. Moreover the resonances have i) different linewidths, as one

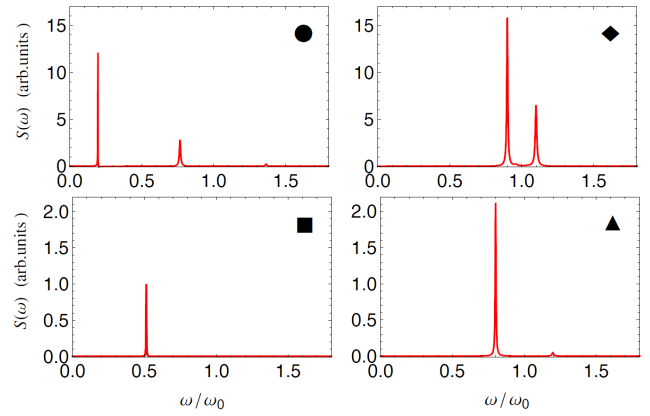


FIG. 4: (color online) Emission spectra calculated for couplings and temperatures corresponding to the markers in Fig. 2 and for $\gamma_a = \gamma_x = 0.01\omega_0$. Spectra heights are normalized by the maximum value of the lowest temperature spectrum (square marker).

can see from the definition of the damping rates and ii) different heights. The latter is mainly a consequence of the thermal feeding. For a fixed temperature, the thermal occupation of a spectral resonance (i.e. its height) is determined by $\bar{n}(\omega, T)$ that increases as the frequency ω of the resonance decreases. The presence of two different decay times in the example with the dot marker becomes apparent via the different linewidths of the resonances contributing to the signal, see Fig. 4a.

Finally we observe that the effects described here could also be measured by populating the system with a quasithermal field distribution realized by mixing a fixed frequency microwave tone with noise sources of different bandwidths [21].

Acknowledgements - This work is part of the Emmy Noether project HA 5593/1-1 and the CRC 631, both funded by the German Research Foundation, DFG.

-
- [1] M. Planck, in *Nobel Lectures, Physics 1901-1921*, Elsevier Publishing Company, (1967).
 - [2] R. Hanbury Brown and R. Q. Twiss, *Nature* **177**, 27 (1956); *Proc. Roy. Soc. (London)* **A242**, 300 (1957); **A243**, 291 (1957).
 - [3] R. J. Glauber, *Phys. Rev.* **130**, 2529 (1963).
 - [4] R. J. Glauber, *Rev. Mod. Phys.* **78**, 1267 (2006).
 - [5] A. V. Shchegrov, K. J., R. Carminati, and J.-J. Greffet *Phys. Rev. Lett.* **85**, 1548 (2000).
 - [6] J.-J. Greffet, R. Carminati, K. Joulain, J-P Mulet, S. Mainguy, and Y. Chen, *Nature* **416**, 61 (2002).
 - [7] G. Günter, A.A. Anappara, J. Hees, A. Sell, G. Biasiol, L. Sorba, S. De Liberato, C. Ciuti, A. Tredicucci, A. Leitenstorfer, and R. Huber, *Nature* **458**, 178 (2009).
 - [8] T. Niemczyk, F. Deppe, H. Huebl, E.P. Menzel, F. Hocke, M.J. Schwarz, J.J. Garcia-Ripoll, D. Zueco, T. Hümmer, E. Solano, A. Marx, and R. Gross, *Nat. Phys.* **6**, 772

- (2010).
- [9] Y. Todorov, A.M. Andrews, R. Colombelli, S. De Liberato, C. Ciuti, P. Klang, G. Strasser, and C. Sirtori, Phys. Rev. Lett. **105**, 196402 (2010).
 - [10] T. Schwartz, J. A. Hutchison, C. Genet, and T. W. Ebbesen, Phys. Rev. Lett. **106**, 196405 (2011).
 - [11] A.J. Hoffman, S.J. Srinivasan, S. Schmidt, L. Spietz, J. Aumentado, H.E. Türeci, A.A. Houck, Phys. Rev. Lett. **107**, 053602 (2011).
 - [12] G. Scalari, C. Maissen, D. Turcinkova, D. Hagenmuller, S. De Liberato, C. Ciuti, C. Reichl, D. Schuh, W. Wegscheider, M. Beck, and J. Faist, Science **16**, 1323 (2012).
 - [13] H. J. Carmichael, *Statistical Methods in Quantum Optics 1*, 2nd ed., Springer, (2000); *Statistical Methods in Quantum Optics 2*, Springer, (2008).
 - [14] F. Beaudoin, J. M. Gambetta, and A. Blais, Phys. Rev. A **84**, 043832 (2011).
 - [15] S. De Liberato, D. Gerace, I. Carusotto, and C. Ciuti, Phys. Rev. A **80** 053810 (2009).
 - [16] A. Ridolfo, M. Leib, S. Savasta and M. J. Hartmann, Phys. Rev. Lett. **109**, 193602 (2012).
 - [17] A. Wallraff, D.I. Schuster, A. Blais, L. Frunzio, R.-S. Huang, J. Majer, S. Kumar, S.M. Girvin and R.J. Schoelkopf, Nature **431**, 162 (2004).
 - [18] J. Q. You and F. Nori, Nature **474**, 589 (2011).
 - [19] E.P. Menzel, F. Deppe, M. Mariani, M. Á. Araque Caballero, A. Baust, T. Niemczyk, E. Hoffmann, A. Marx, E. Solano, and R. Gross, Phys. Rev. Lett. **105**, 100401 (2010).
 - [20] D. Bozyigit, C. Lang, L. Steffen, J. M. Fink, C. Eichler, M. Baur, R. Bianchetti, P. J. Leek, S. Filipp, M. P. da Silva, A. Blais, and A. Wallraff, Nature Phys. **7**, 154 (2011).
 - [21] C. Lang, D. Bozyigit, C. Eichler, L. Steffen, J.M. Fink, A.A. Abdumalikov, Jr., M. Baur, S. Filipp, M.P. da Silva, A. Blais, and A. Wallraff, Phys. Rev. Lett. **106**, 243601 (2011).
 - [22] M. Mariani, E.P. Menzel, F. Deppe, M. Á. Araque Caballero, A. Baust, T. Niemczyk, E. Hoffmann, E. Solano, A. Marx, and R. Gross, Phys. Rev. Lett. **105**, 133601 (2010).
 - [23] S. Ashhab and F. Nori, Phys. Rev. A **81**, 042311 (2010).
 - [24] P. Nataf, and C. Ciuti, Phys. Rev. Lett. **104**, 023601 (2010).
 - [25] C. Emary and T. Brandes, Phys. Rev. A **69**, 053804 (2004).
 - [26] H.-P. Breuer and F. Petruccione, *The Theory of Open Quantum Systems*, Oxford University Press (2006).
 - [27] C. W. Gardiner and P. Zoller, *Quantum Noise*, Springer-Verlag, (2000).
 - [28] The expectation value of a generic one-time operator $\mathcal{O}(t)$ can be calculated as $\text{Tr}[\mathcal{O}\rho(t)]$.
 - [29] see supplementary material
 - [30] V. E. Manucharyan, J. Koch, L. I. Glazman, and M. H. Devoret, Science **326**, 113 (2009).
 - [31] Notice that Eq. (1) does not contain the so called \mathbf{A}^2 term, that is the term associated to the squared electromagnetic vector potential term. This term is often neglected, however its absence in Eq. (1) is not an approximation when considering a system that contains an artificial atom (*fluxonium* [30]) made of a Josephson junction coupled inductively to a resonator.

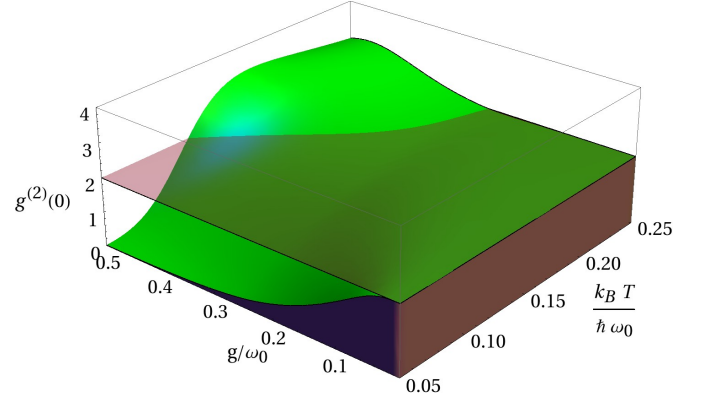


FIG. 5: (color online) $g^{(2)}(0)$ calculated for two TLS coupled with a single cavity mode.

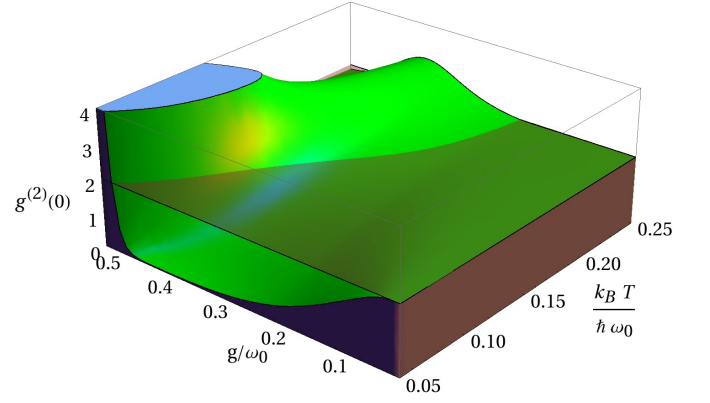


FIG. 6: (color online) $g^{(2)}(0)$ calculated for three TLS coupled to a single cavity mode.

SUPPLEMENTARY MATERIAL

In this section we report calculations of $g^{(2)}(0)$ for many TLS coupled to a single cavity mode, and for a single TLS coupled to two cavity modes. The latter case is of particular interest because of the unavoidable coupling of the TLS to higher modes that is often present in a real experimental setup. In each graph we plot $g^{(2)}(0)$ as function of the temperature and of coupling strength, imposing $\omega_0 = \omega_x$ and $T_a = T_x$, i.e. at thermal equilibrium. We show moreover in all the graphs the plane $g^{(2)}(0) = 2$ to highlight the differences to the standard ME calculation which applies a RWA. The generalization of our model to many TLS is straightforward, and described by the Hamiltonian $H = \omega_0 a^\dagger a + \sum_j \omega_x^{(j)} \sigma_j^+ \sigma_j^- + (a + a^\dagger) \sum_j g^{(j)} (\sigma_j^- + \sigma_j^+)$.

Figs. 5, 6 and 7 show the feasibility to reach a robust quantum regime, characterized by the strong antibunching, that persists even in presence of many TLSs. It is worth to notice the onset of a significant superbunching for higher coupling strength. This is due to the degeneracy of the involved energy levels, that increase with the

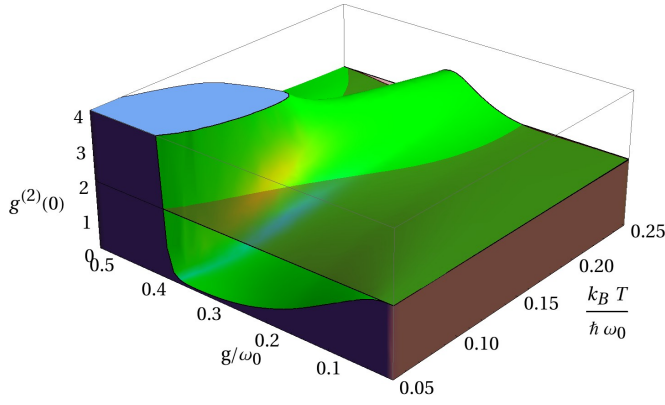


FIG. 7: (color online) $g^{(2)}(0)$ calculated for four TLS coupled to a single cavity mode.

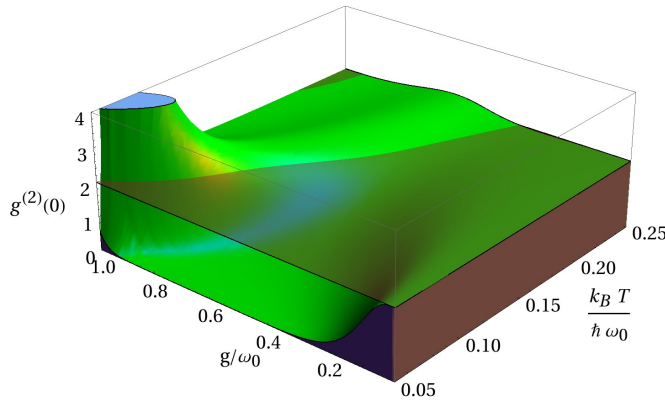


FIG. 8: (color online) $g^{(2)}(0)$ calculated for a TLS coupled to two cavity modes.

number of TLSs.

Fig. 8 in turn shows the thermal $g^{(2)}(0)$ calculated for a single TLS coupled with two cavity modes as described by the Hamiltonian $H = \omega_0^{(1)} a_1^\dagger a_1 + \omega_0^{(2)} a_2^\dagger a_2 + \omega_x \sigma^+ \sigma^- + [g^{(1)}(a_1 + a_1^\dagger) + g^{(2)}(a_2 + a_2^\dagger)](\sigma^- + \sigma^+)$. In particular, for this latter calculation we used a second bare cavity mode with frequency $\omega_0^{(2)} = 2\omega_0^{(1)}$ and a coupling with strength $g^{(2)} = 2g^{(1)}$. Such ratios of coupling strength appear for example in circuit QED experiments [8]. It is worth to notice the enhancement of the antibunching even though we consider a second bosonic mode. The explanation of such scenario is that the presence of the second cavity mode is compensated by the stronger coupling that effectively increase the nonlinearity of the whole system.